*International Journal of Thermophysics, Vol. 24, No. 5, September 2003 (© 2003)*

# A Quasi-Steady State Technique to Measure the Thermal Conductivity[1]

**U. Hammerschmidt**[2]

A new method is developed for the measurement of thermal conductivity. It combines characteristic advantages of steady-state and transient techniques but avoids major drawbacks of both these classes of methods. On the basis of a simple transient hot wire (THW) or transient hot-strip (THS) arrangement, a direct indicating thermal-conductivity meter is realized by adding only one temperature sensor. After a short settling time during which all transients die out, the instrument operates under quasi-steady state conditions. No guard heaters are required because outer boundaries are free to change with time. The instrument's uncertainty is provisionally estimated to be 3%.

**KEY WORDS:** quasi-steady state technique; thermal conductivity; transient hot strip, transient hot wire.

## 1. INTRODUCTION

In principle, the measurement of the thermal conductivity $\lambda$ requires a knowledge of the local *or* time-dependent temperature distribution within the material under test which provides the potential for heat transport. When the temperature, $T(\vec{r})$, varies only locally, the thermal conductivity is calculated from Fourier's first law. Time-dependent temperature profiles, $T(t)$, are governed by Fourier's second law, a second-order partial differential equation.

A one-dimensional temperature field, $T(x)$, which can be characterized by at least two thermometers at different fixed positions, $x_1$ and $x_2$, is used for steady-state measurements. Realizing a static temperature field and

[1] Paper presented at the Sixteenth European Conference on Thermophysical Properties, September 1–4, London, United Kingdom.

[2] Physikalisch-Technische Bundesanstalt, Bundesallee 100, D-38116 Braunschweig, Germany. E-mail: ulf.hammerschmidt@ptb.de



0195-928X/03/0900-1291/0 © 2003 Plenum Publishing Corporation

maintaining it at thermal equilibrium not only requires a heat source and a heat sink but also additional guard heaters. The latter have to be adjusted carefully during settling time and controlled permanently over a long period in time (cf., e.g., Ref. 1).

For transient measurements, generally just one thermometer is needed to characterize the time-dependent temperature $T(t)$ at a known position $r$ within the specimen. In the transient hot wire (THW) and transient hot-strip (THS) techniques, an embedded heat source, a thin wire or a metal strip, respectively, works as a "self-heated thermometer." Upon a step change in its electrical input, it monitors the temperature excursion of the time-dependent temperature field $T(\vec{r} = \vec{r}_1, t)$. The specimen is used as the heat sink of the system. Instruments according to these techniques are much faster than steady-state ones, but the reliability of the results depends strongly on the proper observation of the initial and boundary conditions (cf., e.g., Refs. 1 to 3).

To avoid the drawbacks of both instrument classes mentioned, their characteristic principles of operation were brought together. Based on the very simple setup of a hot-strip or hot wire instrument, only one additional thermometer is needed to realize the fast quasi-steady state operating instrument described below.

This paper can be divided into two parts. The first part starts with an overview of the basic theories of the closely related THW and THS techniques. Their working equations for the quasi-steady state mode are then derived in the framework of an ideal model of unbounded specimens. In practice, however, the (finite) specimen is subject to a prescribed temperature or heat flux distribution at its outer surfaces. Therefore, the theory is extended. For the three different types of linear boundary conditions, quasi-steady state working equations are introduced. In the second part, experimental results are presented for the candidate reference material polystyrene, measured at two different boundary conditions.

## 2. THEORY

The ideal quasi-steady state mode works with a resistive heat source that is entirely embedded inside the specimen without any thermal contact resistance. The electrical input power is totally converted into a rate of heat flow that is liberated immediately and exclusively to the finite (!) specimen. The specimen is free to lose heat to the surroundings as long as boundary conditions vary with time only. The temperature field of the specimen may be far from thermal equilibrium; the field's profile should be cylindrical. Thus, a line- or strip-shaped source is considered in an arrangement that is most similar to the known THW or THS setup.

First, the working equation for the quasi-steady state mode for a hot wire inside an unbounded specimen will be derived based on the existing ideal theory. Unfortunately, there is no appropriate solution at hand for the THS method. Therefore, it will be demonstrated by the use of similarity reasons that the results obtained may be extended to the closely related THS technique without major restrictions. Secondly, the system's thermal response to an outer surface of a finite specimen will be analyzed. Most cases of practical use deal with one of three different kinds of boundary conditions. These will be treated mathematically with expressions given in terms of Bessel functions. These solutions are complete and exact but can be handled only numerically. Therefore, closed form solutions for limiting cases are derived which are most advantageous for practical use.

## 2.1. Quasi-Steady State Mode of a Line Source

The theoretical background of the THW and the THS techniques is presented in detail elsewhere (cf., e.g., Refs. 1–10). Starting from the ideal physical model of an infinitely long line heat source ($z \to \infty$) that is perfectly embedded inside an unbounded homogeneous isotropic medium at ($x = 0$, $y = 0$), the temperature excursion from the initial temperature $T_0$ at any position ($x$, $y$) and any time $t$ is obtained by integration of

$$T_w(x, y, t) - T_0 = \Delta T_w(x, y, t) = \frac{\Phi_0}{4\pi L\lambda} \int_0^t \exp\left(-\frac{x^2+y^2}{4a(t-t')}\right) \frac{dt'}{t-t'} \tag{1}$$

with regard to $t'$. This results in

$$\Delta T_w(r, t) = -\frac{\Phi_0}{4\pi L\lambda} \mathrm{Ei}\left(-\frac{r^2}{4at}\right), \qquad r^2 = x^2+y^2 \tag{2}$$

Here, the strength of the heat source is given by $\Phi_0/L$. The thermal conductivity and thermal diffusivity of the surrounding medium, the heat sink, are denoted by $\lambda$ and $a$, respectively. The argument of the exponential integral, $-\mathrm{Ei}(-\delta)$, is briefly given as $1/\tau_w^2$ where

$$\tau_w = \sqrt{4at}/r \tag{3}$$

is called the non-dimensional time. For $1/\tau_w^2 \ll 1$, Eq. (2) may be approximated by

$$\Delta T_w(r, t) = \frac{\Phi_0}{4\pi L\lambda}\left[-\gamma + \ln\left(\frac{4at}{r^2}\right)\right] \tag{4}$$

which is the commonly used quasi-linear working equation of the THW technique. Here, $C = \exp \gamma$ ($\gamma$: Euler constant).

With Eq. (4), the individual temperatures $T_{W1}$ and $T_{W2}$ of two thermometers at different positions $r_1$ and $r_2 = \varepsilon r_1$, ($\varepsilon > 1$), can immediately be written as

$$T_{W1} = T_W(r_1, t) = \frac{\Phi_0}{4\pi L\lambda}\left(\ln t + \ln \frac{4a}{Cr_1^2}\right) + T_0 \tag{5}$$

$$T_{W2} = T_W(r_2, t) = \frac{\Phi_0}{4\pi L\lambda}\left(\ln t + \ln \frac{4a}{C(\varepsilon r_1)^2}\right) + T_0 \tag{6}$$

Equation (4) becomes valid not before $\tau_W(r) \approx 6$ [9]. Since the nondimensional time is given in terms of the position of the individual temperature stations, $r_i$, Eqs. (5) and (6) become valid at different times, $[\tau_W(\varepsilon r_1)]^{-2} > [\tau_W(r_1)]^{-2}$. Their mutual time lag depends on $\varepsilon^2$.

Subtracting $T_{W2}$ from $T_{W1}$ eliminates from the model not only the thermal diffusivity $a$ but also the time dependence. The resulting stationary working equation for the differential signal $\Delta' T$ governs the *quasi-steady state* mode of a THW measuring process:

$$\Delta' T = T_{W1} - T_{W2} = \frac{\Phi_0}{2\pi L\lambda} \ln \varepsilon \tag{7}$$

For a given strength of the source and a prearranged distance of the temperature stations, $\ln \varepsilon$, the quasi-steady state signal depends only on the thermal conductivity of the sink. Thus, the measurand follows:

$$\lambda = \frac{\Phi_0}{2\pi L\, \Delta' T} \ln \varepsilon \tag{8}$$

This result, of course, is identical with the working equation of the related steady-state radial heat-flow technique [2]. Hence, Eq. (8) is also valid during thermal equilibrium (for full discussion, cf. Section 2.3).

In practice, a quasi-steady state instrument's scale can be marked in terms of the measurand $\lambda$ to realize a direct reading (cf. Figs. 11 or 13). Figure 1 shows a FEM simulation of all three relevant temperatures of a sample of given properties at isothermal boundary conditions. It can be seen that the quasi-steady state mode starts working a little later than the transient mode because of the mutual time shift mentioned above.

Alternatively to the two-thermometer arrangement described, it is sufficient to use only one thermometer in addition to the hot wire. The wire

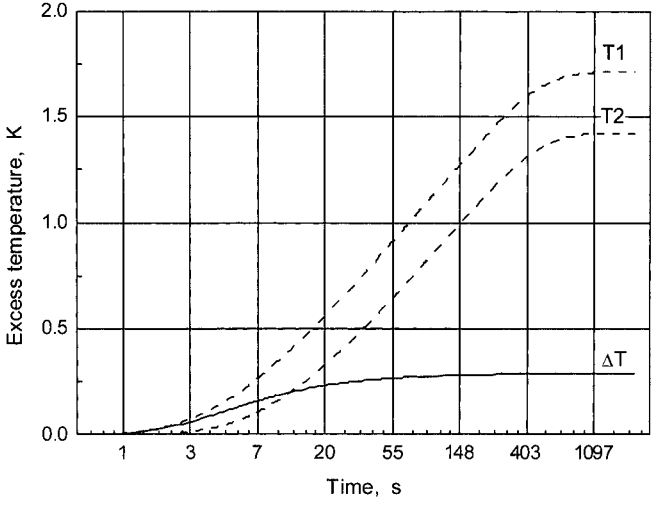


**Fig. 1.** Excess temperature versus time of thermometers T1 and T2 along with quasi-steady state difference, $\Delta T$ (FEM simulation with isothermal boundary conditions).

itself generally acts as a temperature sensor for $T_1$ while $T_2$ is provided by a thermometer at distance $r_2$ from the wire.

As has been shown in Ref. 5, the quasi-linear working equation of the THS technique, Eq. (11), is most similar to Eq. (4). This close correlation gives rise to the assumption that the quasi-steady state should also be possible with an analoguous modification to the THS setup.

## 2.2. Quasi-Steady State Mode of a Strip Source

In order to extend the above results to the THS method, first, a relationship for the temperature distribution of a strip source has to be derived that is expressed in terms of the spatial coordinates $x$ and $y$. In contrast to the THW mathematical model, the THS model characterizes the temperature profile only at a circumferencial line of radius $r = D$ around the $z$-axis [4].

The THS model is based on a strip source of infinite length, $\Delta z \to \infty$, and vanishing thickness, $\Delta x \to 0$, embedded in a homogeneous and isotropic medium. Theoretically, the strip is treated like an array of parallel line sources of full width $D = 2d$ $(-d \leqslant y \leqslant +d)$ [10]. The temperature excursion is governed by

$$\Delta T_S(x, y, t) = \frac{\Phi_0}{4\sqrt{\pi}\, LD\lambda} \int_0^{\sqrt{4at}} \exp\left(-\frac{x^2}{\sigma^2}\right)\left[\operatorname{erf}\left(\frac{y+d}{\sigma}\right) - \operatorname{erf}\left(\frac{y-d}{\sigma}\right)\right] d\sigma \tag{9}$$

where

$$\mathrm{erf}(\delta) = \frac{2}{\sqrt{\pi}} \int_0^{\delta} \exp(-s^2)\, \mathrm{d}s \tag{10}$$

denotes the error function. A two-dimensional time-dependent solution to Eq. (9) can, so far, be obtained only numerically.

By setting $x$ equal to zero, Gustafsson [10] was able to solve this integral analytically in the one-dimensional form $\Delta T(0, y, t)$. By averaging the temperature distribution across the width of the strip to express the mean temperature of the heat source, the second variable, $y$, also vanishes. Thus, the final result, the quasi-linear working equation,

$$\Delta T_{\mathrm{S}}(D, t) = \frac{\Phi_0}{4\pi L\lambda}\left[3 - \gamma + \ln\left(\frac{4at}{D^2}\right)\right], \tag{11}$$

is given in terms of the constant parameter $D$ [5]. By recalling Eq. (4), the similarity between the models of both transient techniques is apparent (cf., Fig. 2). Equation (11) is valid not before $\tau_{\mathrm{S}}(r) \approx 2$.

Obviously, the two-wire-arrangement as described above can be applied analogously by using two strips of different widths $D_1$ and $D_2 = \varepsilon D_1$. Then, the difference in the individual transient temperatures of both strips is the same as given above, Eq. (7). The second approach is the two-thermometer

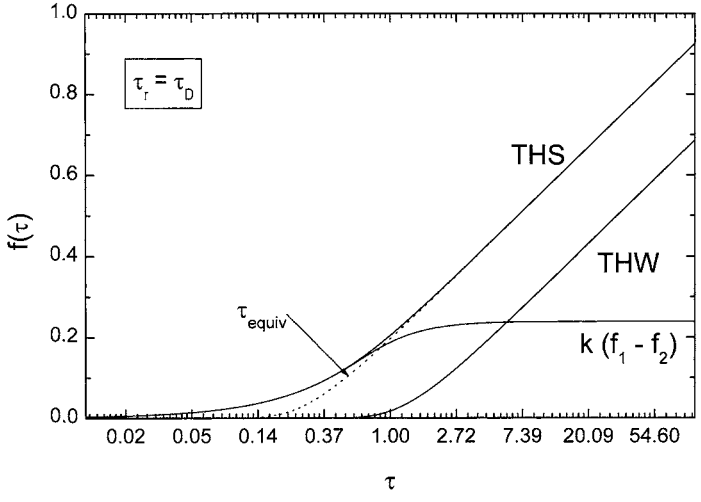


**Fig. 2.** Ideal signals of THW and THS techniques versus nondimensional time.

arrangement consisting of only one strip and two separate temperature stations (cf. Fig. 10). However, derivation of the working equation for this mode of operation is more complex than for the wire: as can be seen from Eq. (11), the non-dimensional time of a THS experiment usually is defined as $\tau_S = \sqrt{4at}/D$. This relation however, is, strictly speaking, no longer a local function like Eq. (3). Thus, the two-dimensional temperature profile generated by a strip cannot be derived either from Eq. (11) or from Eq. (9).

A closer look at the curves of equal temperatures around a line heat source inside an unbounded homogeneous and isotropic medium shows a family of concentric circles (cylinders) that are spread over the $xy$-area as $\ln(1/r^2)$. For a strip source it was pointed out in Ref. 5 that the isothermal curves change their shape from (near-)elliptical to (near-)circular with increasing distance from the source. At $r \geqslant D$ and times $\tau_S^{-2} \ll 1$, the isothermal curves can practically be treated as circles (cf., Eq. (11); this relation is valid only if $D$ represents the radius of a circular isothermal curve.). This heuristic approach is now verified in a more rigorous way than given in Ref. 5.

To derive a first-order approximate solution to Eq. (9), first, Eq. (10) is denoted briefly:

$$\Delta T_S(x, y, t) = \frac{A}{d} \int_0^{\sqrt{4at}} f_x f_y \, d\sigma \tag{12}$$

Secondly, $f_y$, the specific THS term, is rewritten as

$$f_y = \operatorname{erf}\left(\frac{y}{\sigma} + \frac{d}{\sigma}\right) - \operatorname{erf}\left(\frac{y}{\sigma} - \frac{d}{\sigma}\right) = f_{y+} - f_{y-} \tag{13}$$

and expanded to individual Taylor series

$$f_{y+} = \operatorname{erf}\left(\frac{y}{\sigma}\right) + \frac{2}{\sqrt{\pi}} \frac{d}{\sigma} \exp\left(-\frac{y^2}{\sigma^2}\right) - \frac{2}{\sqrt{\pi}} \left(\frac{d}{\sigma}\right)^2 \frac{y}{\sigma} \exp\left(-\frac{y^2}{\sigma^2}\right) + \frac{2}{3\sqrt{\pi}} \left(\frac{d}{\sigma}\right)^3 \left[2\frac{y^2}{\sigma^2} - 1\right] \exp\left(-\frac{y^2}{\sigma^2}\right) + \cdots \tag{14}$$

$$f_{y-} = \operatorname{erf}\left(\frac{y}{\sigma}\right) - \frac{2}{\sqrt{\pi}} \frac{d}{\sigma} \exp\left(-\frac{y^2}{\sigma^2}\right) - \frac{2}{\sqrt{\pi}} \left(\frac{d}{\sigma}\right)^2 \frac{y}{\sigma} \exp\left(-\frac{y^2}{\sigma^2}\right) - \frac{2}{3\sqrt{\pi}} \left(\frac{d}{\sigma}\right)^3 \left[2\frac{y^2}{\sigma^2} - 1\right] \exp\left(-\frac{y^2}{\sigma^2}\right) - \cdots \tag{15}$$

Subtracting term-by-term results in

$$f_{y+} - f_{y-} = \frac{4}{\sqrt{\pi}} \frac{d}{\sigma} \exp\left(-\frac{y^2}{\sigma^2}\right) + \frac{4}{3\sqrt{\pi}} \left(\frac{d}{\sigma}\right)^3 \exp\left(-\frac{y^2}{\sigma^2}\right)^3 \left[2\frac{y^2}{\sigma^2} - 1\right] + \cdots \tag{16}$$

The first two nonzero terms are retained and substituted into Eq. (9):

$$\Delta T_S(x, y, t) \approx \frac{4A}{\sqrt{\pi}} \int_0^{\sqrt{4at}} \exp\left(-\frac{x^2}{\sigma^2}\right) \times \left[\frac{1}{\sigma} \exp\left(-\frac{y^2}{\sigma^2}\right) + \frac{1}{3}\frac{d^2}{\sigma^3}\left(2\frac{y^2}{\sigma^2} - 1\right) \exp\left(-\frac{y^2}{\sigma^2}\right)\right] d\sigma \tag{17}$$

Setting $\sigma = \sqrt{4a(t-t')}$ and recalculating, it finally follows that

$$\Delta T_S(x, y, t) \approx \frac{\Phi_0}{4\pi L\lambda} \int_0^t \exp\left(-\frac{x^2+y^2}{4a(t-t')}\right) \times \left[1 + \frac{1}{3}\frac{d^2}{4a(t-t')}\left(2\frac{y^2}{4a(t-t')} - 1\right)\right] \frac{dt}{t-t'} \tag{18}$$

This relation is now compared with Eq. (1).

The higher order correction term $d^2/\sqrt{4a(t-t')}$ under the integral sign vanishes for $d \to 0$ which is the case for a (single) line source (cf. Eq. (1)), and/or for large times $t$, i.e., small values of $1/\tau_S^2 = d^2/(at)$. In Ref. 5 it has been shown that the latter condition is reasonably well satisfied for distances $r \geqslant 2d = D$ from the center line of the strip, i.e., all isothermal curves $T_i(r_i \geqslant D, t)$ can be regarded as sufficiently circular (cf. Figs. 3 and 4). Thus, Eq. (11) may be rewritten to

$$\Delta T_S(r \geqslant D, t) = \frac{\Phi_0}{4\pi L\lambda}\left[3 - \gamma + \ln\left(\frac{4at}{r^2}\right)\right] \tag{19}$$

Again, the above discussed result, the working equation for the quasi-steady state mode, Eq. (8), can easily be obtained. A finite-element analysis (FEM) confirms Eq. (19).

### 2.3. Boundary Conditions

The quasi-linear working equations, Eqs. (7) and (8), are derived under the assumption of a closed thermodynamic system in which the source is continuously liberating its heat entirely and immediately to the

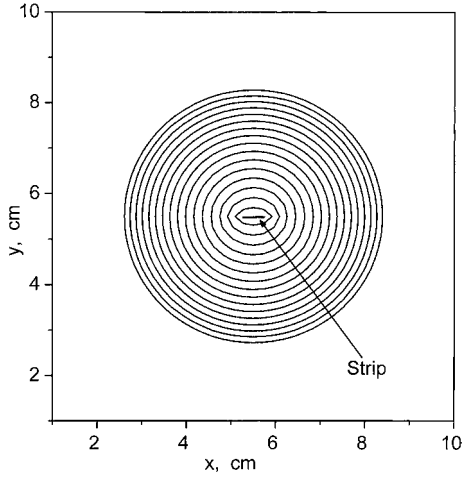


**Fig. 3.** Family of isothermal curves generated by a strip heat source (ideal model).

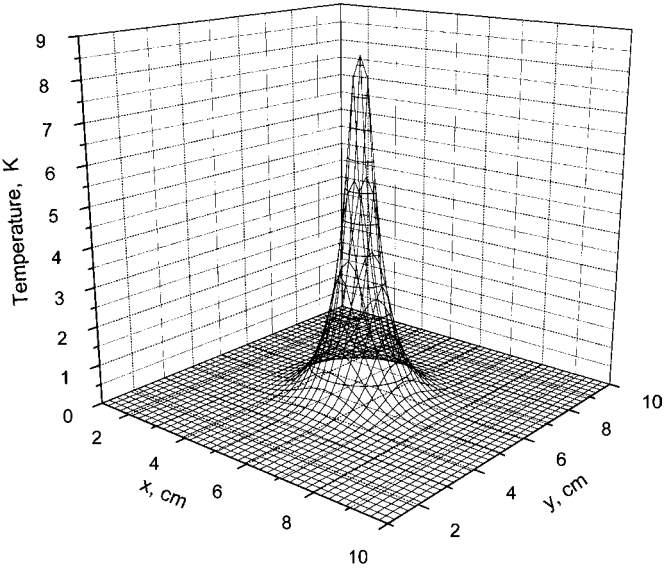


**Fig. 4.** Quasi-three-dimensional temperature profile of a strip source (ideal model).

surrounding sink where it is stored totally. In practice, however, not only the sink (specimen) responds to the heat emitted by the source (wire or strip) but also the source itself and the surroundings of the setup. The source stores heat due to its non-vanishing heat capacity, and the surroundings absorb heat from the outer surfaces of the finite sink. Thus, whenever dealing with finite specimens, boundary conditions have to be taken into account. At its outer surface, $S$, a specimen thermally interacts with the surroundings by conduction, convection, and radiation. Generally, these three effects depend on position and time in a complex way. In transient measurement practice, however, an attempt is made to subject the specimen to steady-state conductive boundary conditions that are either (near-)adiabatic[3] or, in most cases, (near-)isothermal.

To simplify matters, here, it is provided that (1) the temperature difference between the specimen and the surroundings is not great and (2) the surroundings are kept at steady-state conditions. From (1) it follows that the power of temperature that enters the related boundary condition is equal to unity, thus, boundary conditions are linear, i.e., only conductive and convective heat transfer need to be considered. (2) The boundary conditions are homogeneous. Then three different kinds of linear homogeneous boundary conditions have to be examined in conjunction with the quasi-steady state mode:

1. the temperature is prescribed (isothermal): $T = 0$ on $S$ (20)
2. the heat flux is prescribed (adiabatic): $\frac{\partial T}{\partial r} = 0$ on $S$ (21)
3. the convection boundary: $\lambda \frac{\partial T}{\partial r} + \alpha T = 0$ on $S$ (22)

In Eq. (22), $\alpha$ denotes the coefficient of heat transfer.

Most cases of practical interest deal with one of the three ways given to lose heat. The existing theory on the temperature profile of a continuous line source embedded in a cylindrical specimen of finite radius $R$ provides mathematical expressions for all three boundary conditions. These particular solutions to Fourier's second law are exact, but not in closed form. They are given by Tautz [11] in terms of first-kind Bessel functions of zero order and first order, $J_0$ and $J_1$, respectively (see below). By using these equations, the behavior of the quasi-steady state mode can only be calculated numerically and represented graphically. In minimum, twenty terms of the series have to be retained to ensure sufficient convergence. For a

[3] The prefix "near" means "as close as practically possible."

**Table I.** Model Parameters for Numerical Evaluation of Eqs. (23) and (27)

| Quantity | Value |
|---|---|
| $r_1$ | 3.5 mm |
| $r_2$ | 4.5 mm |
| $R$ | 30 mm |
| $L$ | 100 mm |
| $T_0$ | 23 K |
| $\Phi_0$ | 0.2 W |
| $\lambda$ | $1.0\ \mathrm{W \cdot m^{-1} \cdot K^{-1}}$ |
| $a$ | $0.5\ \mathrm{mm^2 \cdot s^{-1}}$ |

given model parameter set (see Table I), the individual temperature excursions of two thermometers, T1 and T2, at different stations have been calculated. These functions are plotted along with their mutual differences, $\Delta T$, in Figs. 5, 6, and 9. It can be seen that, after a relatively short settling time, the quasi-steady state mode not only works during the quasi-linear transient state but also through the long-term states of the three different boundary conditions and their intervening transition phases.

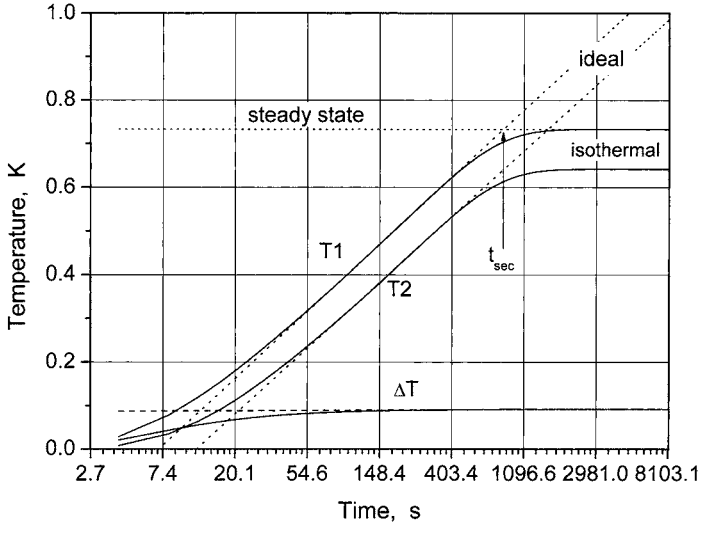


**Fig. 5.** Calculated temperature excursions of two sensors, T1 and T2, at different distances from a line heat source at isothermal boundary conditions (cf. Eq. (23)). $\Delta T$ denotes the quasi-steady state differential signal of both sensors.

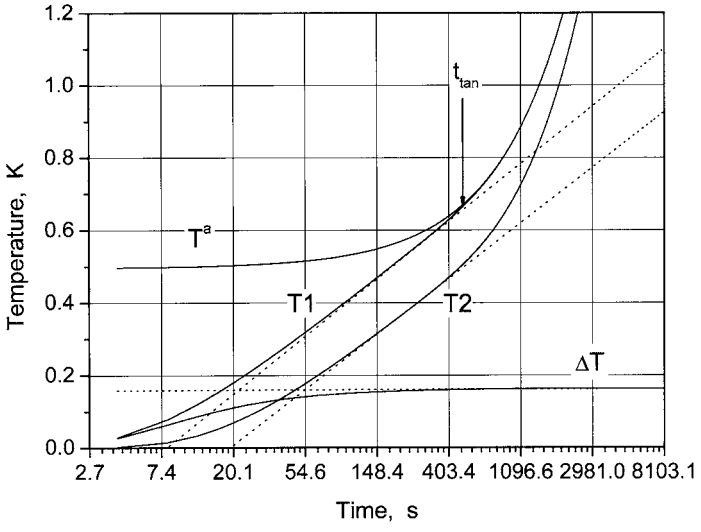


**Fig. 6.** Calculated temperature excursions of two sensores, T1 and T2, at different distances from a line heat source at adiabatic boundary conditions (cf. Eq. (27)). $\Delta T$ denotes the quasi-steady state differential signal of both sensors, $T^a$ is the calorimeter line.

Restricting to the transient and the long-term states, closed form partial solutions are readily at hand to demonstrate the quasi-steady state behavior analytically.

### *2.3.1. Isothermal Boundary*

The temperature, $T_0^i$, of the boundary surface $S$ at a distance $r = R$ from the line source is maintained constant, i.e., the outer surface is open for potential outward heat transfer. In practice, this is (nearly) the case for the specimen to be in good contact with a massive high-conductive metal heat sink of uniform temperature. The internal temperature distribution $T(r, t)$ of the specimen is governed by

$$T^i(r,t) = T_0^i + \frac{\Phi_0}{4\pi L\lambda} \ln\left(\frac{R}{r}\right)^2 - 4\sum_{n=1}^{\infty} \frac{J_0(\mu_n r/R)}{\mu_n^2 J_1^2(\mu_n)} \left[\frac{\Phi_0}{4\pi L\lambda} + \frac{1}{2} T_0^i \mu_n J_1(\mu_n)\right] \exp\left(-\frac{\mu_n^2 at}{R^2}\right) \quad (23)$$

The eigenvalues are $J_0(\mu) = 0$ and $J_1(\mu) = 0$.

From the foregoing result, a closed form solution to the problem stated above can be achieved for the limiting case $t \to \infty$. Then, the sum on the right-hand side vanishes and Eq. (23) reduces to

$$T^{\mathrm{i}}_{\infty} = T^{\mathrm{i}}_{0} + \frac{\Phi_0}{4\pi L\lambda} \ln\left(\frac{R}{r}\right)^2 \tag{24}$$

Obviously, the temperature excursion now does no longer depend on time. Equation (24) represents the working equation of the steady-state mode. This mode becomes apparent when the *entire* rate of heat flow generated by the source leaves the cylindrical specimen on $S$, $\Phi_0 = \Phi_{\mathrm{S}}$.

For the early stage of the temperature rise considered, as long as the rate of heat flow passing through $S$ is negligible, $\Phi_{\mathrm{S}} \approx 0$, there is practically no dependence on the boundaries. As has been shown elsewhere (e.g., Refs. 11 and 12), virtually, this is the case of an infinite specimen, represented by Eq. (2) and Eq. (4), respectively.

In summary, there are two analytical expressions, Eqs. (24) and (4), that, although piecewise valid, closely approximate the internal temperature distribution:

$$\Delta T^{\mathrm{i}}(r, t) \approx \begin{cases} \dfrac{\Phi_0}{4\pi L\lambda}\left(\ln\left(\dfrac{4at}{r^2}\right) - \gamma\right) & \text{for} \quad t_{\min} < t < t_{\mathrm{sec}} \\ \dfrac{\Phi_0}{4\pi L\lambda} \ln\dfrac{R^2}{r^2} & \text{for} \quad t > t_{\mathrm{sec}} \end{cases} \tag{25}$$

For the characteristic time $t_{\mathrm{sec}}$, Healy et al. [11] give an approximation by constructing a point (of intersection) that is common to both functions, Eq. (25) (cf. Fig. 5):

$$t_{\mathrm{sec}} = \frac{C}{4}\frac{R^2}{a} \tag{26}$$

The behavior of the quasi-steady state mode at isothermal boundaries can now be evaluated analytically: by subtracting the temperatures, $\Delta T^{\mathrm{i}}(r, t)$, at two different positions, $r = r_1$ (first thermometer) and $r = \varepsilon r_1$ (second thermometer), Eq. (7) is regained individually for both intervals of Eq. (25).

As has already been pointed out, there is no appropriate solution for a THS experiment. Here, only an FEM analysis can furnish (numerical) results. Figure 1 shows that the quasi-steady state behavior is the same as for the wire (cf. Section 2.2).

### 2.3.2. *Adiabatic Boundary*

When no heat enters or leaves the outer surface $S$ of a specimen, $\Phi_S = 0$, boundary conditions are described as adiabatic. In practice, this is (nearly) the case for the entire specimen to be surrounded by an effective thermal insulation (e.g., fiber board, vacuum). The temperature excursion is governed by:

$$T^a(r,t) = T_0^a + \frac{\Phi_0}{4\pi L\lambda}\left[\frac{4at}{R^2} + \frac{r^2}{R^2} + \ln\left(\frac{R}{r}\right)^2 - \frac{3}{2} - 4\sum_{n=1}^{\infty}\frac{J_0(\mu_n r/R)}{\mu_n^2 J_0^2(\mu_n)}\exp\left(-\frac{\mu_n^2 at}{R^2}\right)\right] \tag{27}$$

The eigenvalues are the same as given above. Again, for times $t \to \infty$, the sum on the right hand side vanishes:

$$T_\infty^a = T_0^a + \frac{\Phi_0}{4\pi L\lambda}\left[\frac{4at}{R^2} + \frac{r^2}{R^2} + \ln\left(\frac{R}{r}\right)^2 - \frac{3}{2}\right] \tag{28}$$

As demonstrated by Fig. 7, this equation represents the (calorimeter-) line of slope,

$$p = \frac{\Phi_0}{4\pi L\lambda}\frac{4a}{R^2} \tag{29}$$

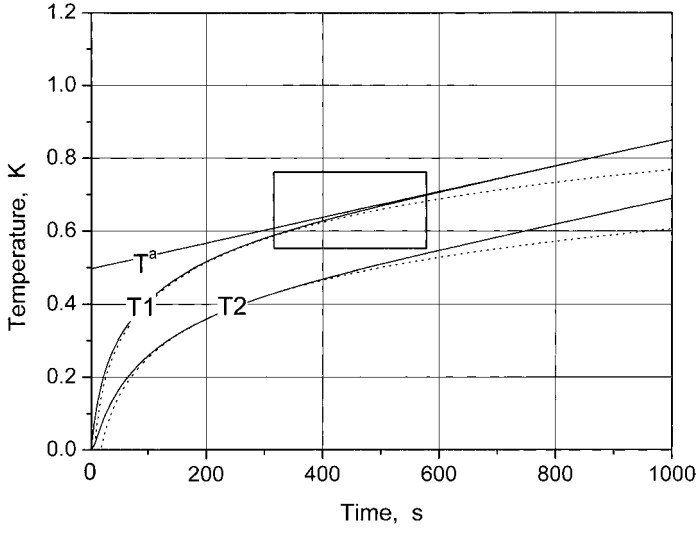


**Fig. 7.** Calculated temperature excursions of two sensors, T1 and T2, at different distances from a line heat source at adiabatic boundary conditions, plotted versus linear time. The dotted lines indicate the ideal case. The curve, $T^a$, is the calorimeter line (see text).

and intercept,

$$q = T_0^{\mathrm{a}} + \frac{\Phi_0}{4\pi L\lambda}\left[\frac{r^2}{R^2} + \ln\left(\frac{R}{r}\right)^2 - \frac{3}{2}\right] \tag{30}$$

Obviously, during the long-term behavior (1) the temperature no longer increases with $\ln t$ but linearly with time and (2) the slope, $p$, no longer depends on the position, $r$, of the thermometer (cf. Eq. (2)) but on the radial size, $R$, of the specimen. As expected, the setup now works like an adiabatic calorimeter. With $a/\lambda = \rho c_{\mathrm{p}}$ and $V = \pi R^2 L$:

$$p = \frac{\Phi_0}{mc_{\mathrm{p}}} \Rightarrow c_{\mathrm{p}} = \frac{\Phi_0}{mp} \tag{31}$$

Here, $m$ denotes the specimen mass and $c_{\mathrm{p}}$ is supposed to be constant.

In summary, it may be stated that the piecewise valid function

$$\Delta T^{\mathrm{a}}(r, t) \approx \begin{cases} \dfrac{\Phi_0}{4\pi L\lambda}\left(\ln\left(\dfrac{4at}{r^2}\right) - \gamma\right) & \text{for} \quad t_{\min} < t < t_{\tan} \\ \dfrac{\Phi_0}{4\pi L\lambda}\left(\dfrac{4at}{R^2} + \ln\dfrac{R^2}{r^2} + \dfrac{r^2}{R^2} - \dfrac{3}{2}\right) & \text{for} \quad t > t_{\tan} \end{cases} \tag{32}$$

sufficiently approximates the temperature field considered, except for the transition phase. The characteristic time $t_{\tan}$ can be obtained as follows:

The transition of the temperature function from the logarithmic, $T(\ln t)$, to the linear, $T(t)$, rise during an experiment under adiabatic boundary conditions certainly is continuous and smooth. This behavior can be shown by a graphical representation of Eqs. (27) and (28) (cf. Figs. 6, 7, and 8). Though both partial functions of Eq. (32) do not share one or more common points, there is one single point, $(t_{\tan}, T)$, of each of the functions whose individual slopes, $\partial T/\partial t$, are equal:

$$\frac{1}{t_{\tan}} = \frac{4a}{R^2} \Leftrightarrow t_{\tan} = \frac{R^2}{4a} \tag{33}$$

This condition for the upper end point of the quasi-linear interval in time is more rigorous than Eq. (26) because $C > 1$ (cf. Fig. 9).

Calculating once more the temperature difference of any two temperature stations $r_1$, $r_2 = \varepsilon r_1 < R$ from Eq. (32b) yields:

$$\Delta' T^{\mathrm{a}} = \frac{\Phi_0}{2\pi L\lambda}\left(\ln\varepsilon + \frac{r_1^2(1-\varepsilon^2)}{2R^2}\right) \tag{34}$$

This is the known result for the quasi-steady state mode plus an additional term, $r^2(1-\varepsilon^2)/2R^2$, that is negative because $\varepsilon > 1$. With further knowledge of its constituents, this term however, can easily be corrected for. It may even be ignored when the distance between both thermometers is adjusted small compared with the sample radius. Figure 8 shows that here again, the quasi-steady state mode is preserved during the transition phase.

Calculated for the same parameters as above, Fig. 9 summarizes the results obtained for the quasi-steady state mode at isothermal and adiabatic boundary conditions.

*2.3.3. Convection Boundary*

At the boundary surface $S$, convection is present into a medium at temperature $T_A$. In practice, this is the case for a specimen that is immersed in a well-stirred thermostated bath. The exact solution can once more be found in Ref. 11:

$$T^c(r,t) = T_A + \frac{\Phi_0}{4\pi L\lambda}\left[\frac{2}{\alpha R} + \ln\left(\frac{R}{r}\right)^2\right] - \sum_{n=1}^{\infty} \frac{\frac{\Phi_0}{\pi L\lambda} + 2T_A\mu_n J_1(\mu_n)}{\mu_n^2[J_0^2(\mu_n)+J_1^2(\mu_n)]} J_0\left(\mu_n \frac{r}{R}\right)\exp\left(-\frac{\mu_n^2 at}{R^2}\right) \tag{35}$$

with

$$\mu_i = \frac{1}{\alpha R}\frac{J_0(\mu_i)}{J_1(\mu_i)}. \tag{36}$$

Again, the sum vanishes for $t \to \infty$ and in this convection limiting case the resultant temperature is obtained as

$$T_\infty^c = T_A + \frac{\Phi_0}{4\pi L\lambda}\left(\frac{2}{\alpha R} + \ln\frac{R^2}{r^2}\right). \tag{37}$$

For large values of the coefficient of heat transfer, $\alpha$, the related term vanishes and Eq. (24) is regained, i.e., the steady-state mode.

It is apparent now that the quasi-steady state mode works at convective boundaries as well as at the other two boundaries discussed above.

## 3. EXPERIMENTS

As has already been pointed out, there are different promising arrangements to realize the quasi-steady state mode of operation. Experiments have been performed using (1) a hot wire cell of 150 mm in length that

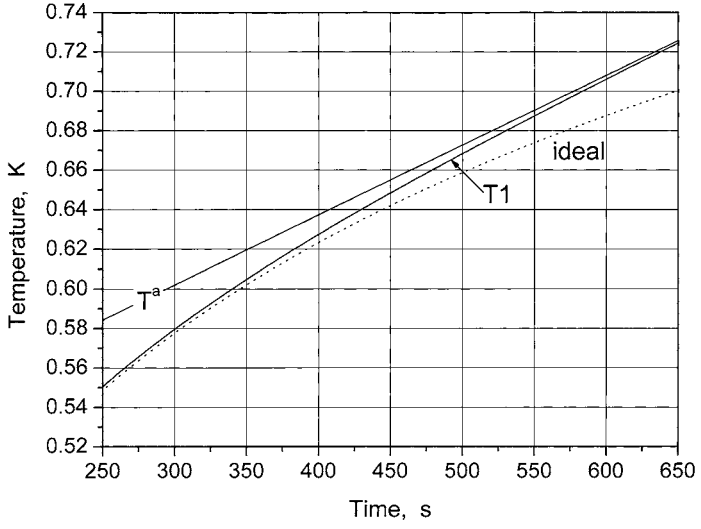


**Fig. 8.** (Insert graph of Fig. 7.) Transition temperature curve from the ideal behavior to the adiabatic limiting case for sensor T1.

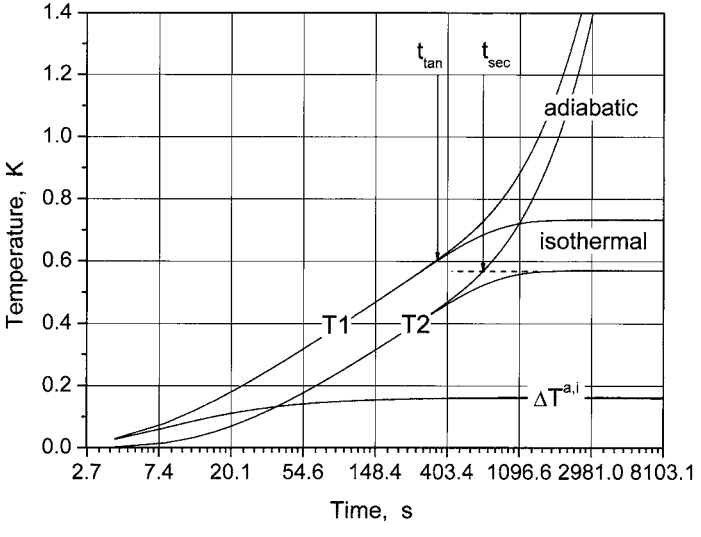


**Fig. 9.** Calculated temperature excursions of two sensors, T1 and T2, at adiabatic (cf. Eq. (23)) and isothermal (cf. Eq. (27)) boundary conditions, respectively. $\Delta T^{a,i}$ indicates the quasi-steady state signal for both cases (cf. Eq. (7)).

contains an additional cold wire at a distance $r_2 = 4.5$ mm [10] and (2) a THS arrangement where two parallel platinum (cold) wires ($r_0 = 0.005$ mm) were added as the thermometers T1 and T2. For the latter setup, a nickel strip of $D = 3$ mm, $L = 100$ mm, and a thickness $v = 5$ µm was used. The temperature sensors are fixed precisely at distances $r_1 = 3.5$ mm and $r_2 = 4.5$ mm, respectively, from the long axis of the strip. The measurements were performed first at near-isothermal (Figs. 10 and 11) and than at near-adiabatic boundary conditions (Figs. 12 and 13) on the candidate reference material polystyrene, PS158K, manufactured by BASF AG. The signals were evaluated using the working equations Eqs. (7) and (8). In Figs. 10 and 12 the THS signals are plotted versus linear and logarithmic time, respectively. Figures 11 and 13 show the resulting differential curves as thermal conductivity vs. time. As has been predicted this kind of signal can be used to build an indicating thermal conductivity meter.

The quasi-steady state mode results were verified against those obtained from guarded hot-plate measurements on samples cut from the same stock. A first estimate of the uncertainty yields 3% at $k = 2$ for the new technique.

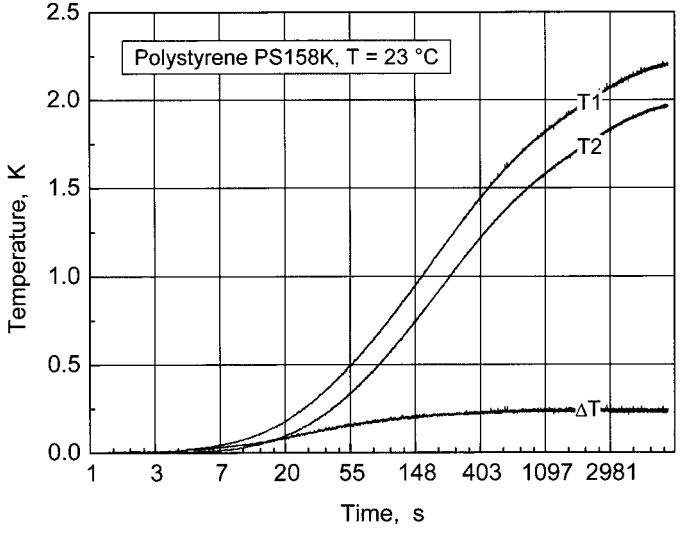


**Fig. 10.** Experimental quasi-steady state mode signal, $\Delta T$, and related individual temperature signals, T1 and T2, of two cold wires vs. $\ln t$ measured at 23°C on polystyrene, PS158K, at isothermal boundary conditions.

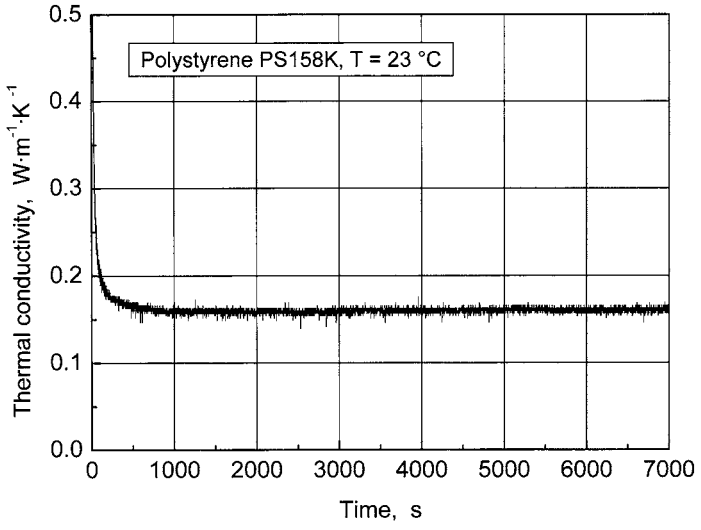


**Fig. 11.** Experimental quasi-steady state mode signal measured at 23°C on polystyrene, PS158K, plotted as thermal conductivity versus time (cf. Fig. 10).

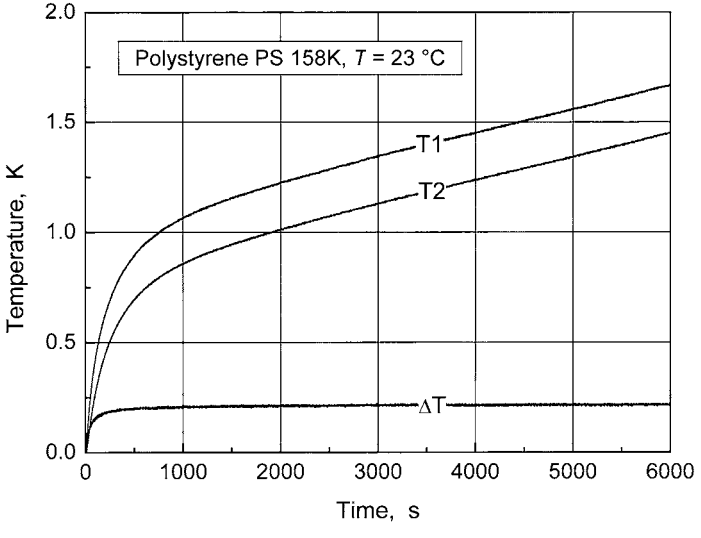


**Fig. 12.** Experimental quasi-steady state mode signal, $\Delta T$, and related individual temperature signals, T1 and T2, of two cold wires vs. $\ln t$ measured at 23°C on polystyrene, PS158K, at adiabatic boundary conditions.

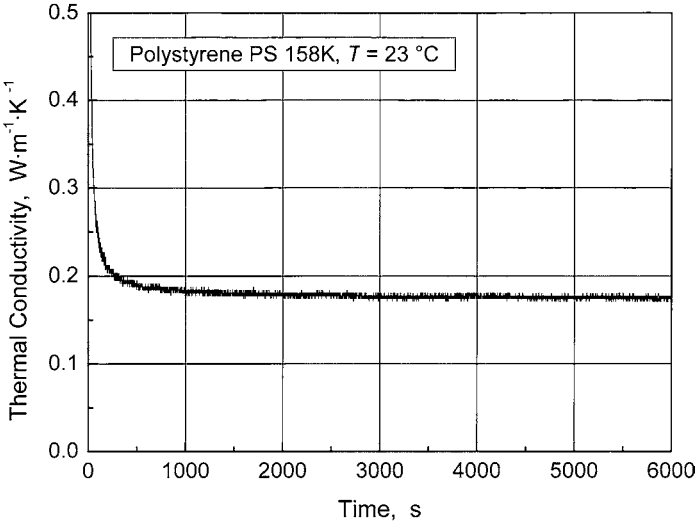


**Fig. 13.** Experimental quasi-steady state mode signal measured at 23°C on polystyrene, PS158K, plotted as thermal conductivity versus time (cf. Fig. 12).

A special hot-strip setup which is applicable for transient, quasi-steady, and steady-state measurements is now under construction (Fig. 14). Between two Kapton foils, there are integrated a hot-strip and two temperature sensors. To generate the prescribed *constant* rate of heat flow the strip is made of manganine because of the constant electrical resistance of this alloy. The two thin parallel "cold" wires are made from platinum. Their active regions are located inside the end-effect free center zone of the temperature profile of the strip.

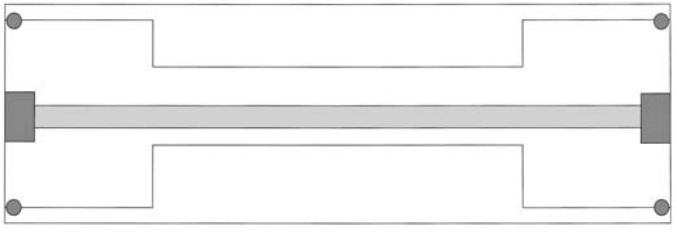

**Fig. 14.** Heater/sensor foil for the quasi-steady state mode of operation. The strip (center) is made from manganine; both temperature sensors (cold wires) are made from platinum.

## 4. SUMMARY

The quasi-steady state mode to the transient hot wire and the transient hot-strip techniques has been introduced for the first time. Only one additional temperature sensor is needed for the THW or THS setup to generate a differential signal which is a time-invariant measure of the thermal conductivity of the material under test. The signal, first settled, practically remains unaffected from homogeneous isothermal, adiabatic, and convective boundary conditions. Thus, the newly developed mode links together the transient with the steady-state technique during the same experiment. It combines the advantages of both standard transient techniques.

To demonstrate the quasi-steady state mode of operation, first the known mathematical model of the THW method is extended slightly to derive the working equation for the new technique. In the case of the THS technique, this short and direct path cannot be followed because of an unsolved integral which governs the two-dimensional temperature field generated by a strip source. By expanding the specific THS term under the integral sign into a series, it can be shown from similarity reasons that the working equation derived is valid for the quasi-steady state THS technique as well. Secondly, it is shown that under the boundary conditions of practical interest the quasi-steady state mode can work without any alterations. Since temperature measurements can be carried out within a center region of the heat source, end effects are eliminated.

The fundamental results obtained theoretically are already confirmed by numerical and experimental investigations. Others will be verified soon.

## REFERENCES

1. H. S. Carslaw and J. C. Jaeger, in *Conduction of Heat in Solids*, 2nd Ed. (Oxford University Press, Oxford, 1959).
2. K. D. Maglic, A. Cezairlyan, and V. E. Peletsky, eds., in *Compendium of Thermophysical Property Measurement Methods, Vol. 1: Survey of Measurement Techniques* (Plenum Press, New York and London, 1984).
3. A. I. Johns, A. C. Scott, J. T. R. Watson, D. Ferguson, and A. A. Clifford, *Philos. Trans. Roy. Soc. London Ser. A* **325**:295 (1988).
4. S. E. Gustafsson, E. Karawacki, and M. N. Khan, *J. Phys. D* **12**:1411 (1979).
5. U. Hammerschmidt, in *Proc. 24th Int. Thermal Cond. Conf.*, P. S. Gaal, ed. (Technomic, Lancaster, Pennsylvania, 1997).
6. W. Sabuga and U. Hammerschmidt, *Int. J. Thermophys.* **16**:557 (1995).
7. S. E. Gustafsson, *Z. Naturforschg.* **22**:1005 (1967).
8. U. Hammerschmidt and W. Sabuga, *Int. J. Thermophys.* **21**:217 (2000).
9. U. Hammerschmidt and W. Sabuga, *Int. J. Thermophys.* **21**:1255 (2000).
10. U. Hammerschmidt, *Int. J. Thermophys.* **23**:975 (2002).
11. H. Tautz, in *Wärmeleitung und Temperaturausgleich* (Verlag Chemie GmbH, Weinheim, 1971).

12. J. J. Healy, J. J. de Groot, and J. Kestin, *Physica C* **82**:392 (1976).
13. R. Model and U. Hammerschmidt, in *Proc. 6th Int. Conf. on Advanced Computational Methods in Heat Transfer, "Heat Transfer 2000,"* Madrid, Spain (2000).
14. U. Hammerschmidt, R. Model, and R. Stosch, "How to Estimate Begin and End of a Transient Event," to be published.